

# A Systematic Simulating Assessment within Reach Greenhouse Gas Target by Reducing PM<sub>2.5</sub> Concentrations in China

Wei Li<sup>1,2\*</sup>, Can Lu<sup>1,2</sup>, Yi Ding<sup>1</sup>

<sup>1</sup>School of Economics and Management, North China Electric Power University,  
No.619 Yonghua Street, Baoding, Hebei 071003, China

<sup>2</sup>Center for Innovation Development and Energy Economics Research, North China Electric Power University,  
Baoding, Hebei 071003, China

*Received: 25 October 2016*

*Accepted: 8 November 2016*

## Abstract

Reducing greenhouse gas emissions and governing pollutant emissions would cause real synergy. Therefore, China has proposed achieving the target of reducing fine particulate matter (PM<sub>2.5</sub>) concentrations to 35 ug/m<sup>3</sup>, as it pollutes the most. The prioritized purpose of this dissertation is aimed at constructing a comprehensive framework by integrating the PM<sub>2.5</sub> target, influencing factors, and countermeasures together to shed some new light on the PM<sub>2.5</sub> governing problem. A computable general equilibrium (CGE) model containing a pollution abatement block is first introduced. Accordingly, four different scenarios about the PM<sub>2.5</sub> target implementation plan are designed for analyzing the impacts on China's macroeconomics, energy demand, and environmental quality, and we establish a PM<sub>2.5</sub> system dynamics model in the principle of system dynamics theory afterward. Subsequently, the model offers six various countermeasures in terms of declining the concentration of PM<sub>2.5</sub> on the basis of the causality diagram. Consequently, the scenario analysis and system simulation results illustrate that the decline in PM<sub>2.5</sub> concentration at annual average rates of 3.07%, 4.61%, and 1.53% from 2016 to 2020, 2021 to 2025, and 2026 to 2030 is significantly beneficial for achieving the PM<sub>2.5</sub> target. Additionally, three effective countermeasures could be approximately reaching the PM<sub>2.5</sub> concentration target in 2030.

**Keywords:** fine particulate matter, computable general equilibrium, system dynamics, scenario analysis, China

## Introduction

Since the implementation of reform and opening-up policy, China's national economic growth has

significantly increased by more than 80-fold [1]. The greenhouse gas issue has attracted increasing attention worldwide, and the Chinese government put forward its Intended Nationally Determined Contributions (INDCs) publically in June 2015 and contributed a lot at the Paris climate conference. Michel den Elzen et al. [2] gave a synthesis research about how China's greenhouse gas emissions reach peak before 2030 from current and

\*e-mail: ncepulw@126.com

enhanced policies. The contradiction between the carrying capacity of the ecological environment and economic growth, accompanied by the rapid growth of our economy, however, has become increasingly remarkable. Strikingly, the haze weather caused by a high concentration level of  $PM_{2.5}$  takes the dominant status among the multitudinous environmental problems in recent years. Simultaneously, large proportions of unfavorable impacts on the development of China's economy, the transformation of energy structure, and the improvement of environmental quality are all exerted by haze. More seriously, this haze weather phenomenon has already threatened the health of humanity. Consequently, an increasing number of studies about air quality has accompanied the haze weather. Mehmet Cetin [3], utilizing bioclimatic comfort mapping methods, showed that Kastamonu has suitable ranges for a bioclimatic comfort zone and has a suitable area for bioclimatic comfort. Hakan Sevik, Mehmet Cetin, and Nur Belkayali [4] measured the amounts of air carbon dioxide in forests and urban areas and evaluated them depending on the season and day or night. They showed that there is a big difference between the amount of carbon dioxide in terms of summer and winter seasons. Cetin and Hakan Sevik [5] attempted to determine the effects of indoor plants on the concentration of  $CO_2$  in an indoor environment under certain light conditions and found that all plants reduced the concentration of  $CO_2$  to a certain extent during the day. Cetin [6] examined and evaluated the changes in the indoor amount of  $CO_2$  in some central exam. The study indicated that air circulation is a must in exam halls to ensure healthy exam environments.

For the sake of highlighting the importance of governing haze weather, China declared that an updated National Ambient Air Quality Standard (NAAQS), which contains the new indicator  $PM_{2.5}$ , was put into effect after 29 February 2012. In addition, limits about the daily average and the annual average concentrations were stipulated as  $75 \mu g/m^3$  and  $35 \mu g/m^3$ , respectively. Furthermore, on 14 February 2013 the U.S. Environmental Protection Agency stated that all cities' annual average concentrations of  $PM_{2.5}$  should reach the standard level of  $35 \mu g/m^3$  by 2030.

In general, the research on the strand of  $PM_{2.5}$  scholarly work could be separated into two aspects: the formation causes and the effects of high  $PM_{2.5}$  concentrations.

In the formation causes aspect, it was proved that the secondary organic aerosol is the main cause, which leads to the formation of  $PM_{2.5}$ , and the contribution of the secondary organic aerosol to  $PM_{2.5}$  in Monterrey has been calculated [7]. Vehicle tailpipe emissions and tobacco smoke are also reasons that format  $PM_{2.5}$ , and the results show that short-duration peak concentrations of up to  $360 \mu g/m^3$  were associated primarily with vehicle tailpipe emissions and tobacco smoke [8]. Amod K. Pokhrel et al. [9] found that biomass fuel stoves without flues were the most significant sources of  $PM_{2.5}$ , followed by kerosene and then LPG stoves. Jia Wang et al. [10] showed that coal combustion, vehicles, coking plants, and biomass burning are the main sources for PAHs and the high concentrations of  $PM_{2.5}$ . Mauro Masiol et al. [11] analyzed

six factors associated with potential sources, including secondary sulfate, ammonium nitrate and combustions, fossil fuels, traffic, industrial, and glassmaking are related to  $PM_{2.5}$ . Dexiang Wang et al. [12] demonstrated the contributions of different sources to primary components and secondary nitrate and sulfate and the contributions of different sources to  $PM_{2.5}$  total mass in Xi'an during the extremely polluted months are: energy 5%, industry 58%, transportation 2%, residential activities 16%, dust 4%, and others – including other components, inexplicit sources, and upwind sources) – 15%. Ray Minjares et al. [13] showed that diesel vehicles offered a greater contribution to the concentration of particulate matter, and Xin Yue et al. [14] inferred that a high level of vehicle emissions occurred mostly in densely populated urban areas and economically well-developed areas and have become one of the most conspicuous and substantial problems to  $PM_{2.5}$  and other pollutants. The combustion of coniferous wood and coal in residential heating and traffic belongs to the biggest emission sources of organic compounds associated with the  $PM_{2.5}$  aerosols [15]. Coal combustion, biomass burning, and long-range transport of windblown dust have great impacts on the concentration of the fine particulate matter [16]. Some models identified gravel-plant, industrial, and port variables as the main sources of  $PM_{2.5}$  [17].

Some quintessential literature related to the impacts of high  $PM_{2.5}$  concentrations can be cited. Cheng [18] found that during winter, the daily variation of  $PM_{2.5}$  in Beijing tracked the pattern of relative humidity. And Nathaniel Gilbraith [19] evaluated the potential for residential demand response to reduce pollutant emissions including particulate matters with experiment samples which focused on New York City. With its adverse effect on social life, fine particulate matter could even cause adverse effects on lifespan, reproduction, locomotion behavior, and intestinal development in the progeny of exposed nematodes [20].  $PM_{2.5}$  also is related to the industrial economy. Michal P. Spilak et al. [21] assessed the association between the concentration levels of particulate matter and building characteristics.

In this paper, a dynamic computable general equilibrium (CGE) model will be applied to reveal the comprehensive impacts of carrying out different plans about the  $PM_{2.5}$  target. The CGE model is derived from the general equilibrium theory by Walras, the model focuses on all of the markets of the economic system and requires that all of the markets be cleared [22]. As an effective policy analyzing tool in economics, the CGE model can well simulate the influence of each economic subjects' performance by the implementation of policy and management measures. With an extensive application, CGE technology can be applied to a great deal of research fields and put forward practical policy suggestions – especially in the fields of international trade, public finance, and climate policy [23-27]. In the  $PM_{2.5}$  sphere, however, typical research should cite that Johannes et al. [28] used the World Scan CGE model to analyze the co-benefits of reduced emissions of air pollutants, which

includes sulfur dioxide (SO<sub>2</sub>), nitrogen dioxide (NO<sub>x</sub>), NH<sub>3</sub>, and PM<sub>2.5</sub> as a by-product of climate policies.

Whereas an urgent awareness on decreasing the concentration of PM<sub>2.5</sub> is rendered increasingly significant considering its intricate formation causes, several works have been studied from this vein to solve this problem [29-31]. We will thus construct a PM<sub>2.5</sub> system dynamics model integrating qualitative analysis with the quantitative calculation together based on system dynamics (SD) theory – a method for modeling, simulating, and analyzing complex systems established by Jay W. Forrester in 1956. This method is recognized as an actual system experiment laboratory, and an overwhelming quantity of fields have been referred to via SD methods. Subsequently, it is especially suitable for solving nonlinear complicated social, economical, and ecological system problems [32-36].

Although both CGE and SD theories have an extensive application in different fields, research combined the two policy analysis tools together to study a comprehensive PM<sub>2.5</sub> policy framework that includes target, factors, and countermeasures. Thus, this paper will employ the dynamic CGE model and SD model together for exploring the PM<sub>2.5</sub> governing policy framework in the initial period of 2016 until 2030.

The remainder of the paper is organized as follows. Section 2 is the methodology of the CGE model. Section 3 is PM<sub>2.5</sub> system dynamics model. Section 4 is results and discussions. Section 5 is conclusions.

## Material and Methods

### CGE Model

The dynamic CGE model in this study stems from the standard CGE model on the basis of Walras's general equilibrium theory. Production, trade, income and expenditure, pollution abatement, investment and saving, household welfare, and equilibrium blocks are included in this CGE model. Agriculture and the construction, manufacturing, service, transportation, coal, oil, natural gas, and electric power industries are chosen as the model's 10 main production sectors. It is assumed that producers take profit maximization as the decision target and consumers take utility maximization as the decision goal simultaneously. In addition, China is modeled as a price taker for its external countries in international trade.

### Production Structure

The production block is a description of each producer's profit-maximizing or cost-minimizing behavior under a certain constraint. We proposed that in this production module each sector has only one producing constant return to scale enterprise, and each enterprise produces only one kind of commodity or service. The model employed five layers of nesting constant elasticity substitution (CES) production function type to describe

the relationship between each production factor. The non-energy intermediate input and the labor-capital-energy beam is located at the highest level of the production block, notably the Leontief linear production function is applied to the intermediate input section; at the second level, it shows the substitution relation between labor and the capital-energy beam; then we discuss how to distribute capital and energy at the third layer; at the fourth level, we subdivided energy into polluted energy and other energy. The polluted energy is the quantity of the energy input from all the other productive sectors, which mainly refers to energy sectors such as coal, natural gas, oil, and electric power – which release exhausted gas emissions like sulfur dioxide (SO<sub>2</sub>) and nitrogen oxides (NO<sub>x</sub>) when a specific productive sector produce one unit of product, while other energy means would not release or release very little exhaust gas emissions during an enterprise's producing and running process. The fifth layer demonstrates the substitution relationship between SO<sub>2</sub> and NO<sub>x</sub> emissions, while the carbon emission is filled at this level. Each of the sector's carbon emissions is equal to multiplying the carbon emission coefficient by carbon dioxide emission of the sector itself. The structure and relationship of each factor can be seen from Fig. 1. Equations (1) to (3) are listed as examples to identify the substitution relationship of the CES function.

$$QA_i = \alpha_i^q [\delta_i^q QVA_i^{\rho_i^q} + (1 - \delta_i^q) QINTA_i^{\rho_i^q}]^{\frac{1}{\rho_i^q}} \quad (1)$$

$$\frac{PINTA_i}{PVA_i} = \frac{\delta_i^q}{(1 - \delta_i^q)} \left( \frac{QVA_i}{QINTA_i} \right)^{(1 - \rho_i^q)} \quad (2)$$

$$PA_i \times QA_i = PVA_i \times QVA_i + PINTA_i \times QINTA_i \quad (3)$$

...where  $QA_i$  stands for gross domestic output, and it constitutes labor-capital-energy beam ( $QVA_i$ ) and intermediate output ( $QINTA_i$ ), which could be expressed through Equation (1). Equation (2) shows that the optimal combination of the two input factors is the first-order condition of the two factors' relative price CES function, where  $PVA_i$  and  $PINTA_i$  are the price of labor-capital-energy beam and intermediate output. Equation (3) illustrates the conditions when each production sector reaches the maximum profit; in other words, this equation indicates that no matter how much the output that each production sector furnishes, it will always maximize profit.

### International Trade Block

Under the background of an open economy, China is a price taker in the international trade business. The goods produced in China domestically are used for two things: to sell on the domestic market and to export abroad. While the commodities sale on the domestic market originated from two modes of supply. One is the goods produced domestically and supply domestically and another is the goods imported from other countries. Due to the incomplete

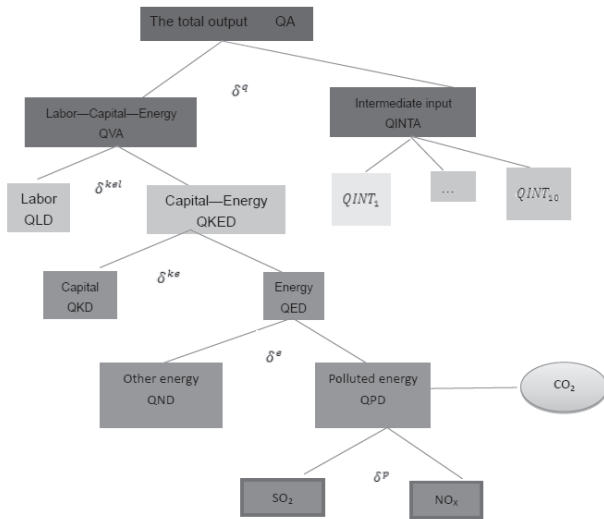


Fig. 1. Five layers' nesting CES production framework.

substitution effect between the domestic productive goods and the import commodities according to Armington assumption, we choose the constant elasticity substitution (CES) function type to indicate the substitution relation between the domestic productive goods and the import commodities. Finally, we select the constant elasticity transformation (CET) function to describe how domestic production is allocated between domestic sold goods and export goods.

$$QA_i = \alpha_i^t [\delta_i^t QDA_i^{\rho_i^t} + (1 - \delta_i^t) QE_i^{\rho_i^t}]^{\frac{1}{\rho_i^t}} \quad (4)$$

$$\frac{PDA_i}{PE_i} = \frac{\delta_i^t}{(1 - \delta_i^t)} \left( \frac{QE_i}{QDA_i} \right)^{(1 - \rho_i^t)} \quad (5)$$

$$PA_i \times QA_i = PDA_i \times QDA_i + PE_i \times QE_i \quad (6)$$

$$QQ_i = \alpha_i^m [\delta_i^m QDC_i^{\rho_i^m} + (1 - \delta_i^m) QM_i^{\rho_i^m}]^{\frac{1}{\rho_i^m}} \quad (7)$$

$$\frac{PDC_i}{PM_i} = \frac{\delta_i^m}{(1 - \delta_i^m)} \left( \frac{QM_i}{QDC_i} \right)^{(1 - \rho_i^m)} \quad (8)$$

$$PQ_i \times QQ_i = PDC_i \times QDC_i + PM_i \times QM_i \quad (9)$$

Equations (4) to (6) describe the CET function substitute relationship of the domestic sold goods ( $QDA_i$ ) and export goods ( $QE_i$ ), and  $PDA_i$  and  $PE_i$  stand for the price of the domestic sold goods and export goods, respectively. Additionally, Equations (7) to (9) show the constitute relationship between domestic productive goods ( $QDC_i$ ) and the import commodities ( $QM_i$ ).  $PDC_i$  and  $PM_i$  mean the price of domestic productive goods and

import goods, respectively. Particularly,  $QQ_i$  represents commodities in the domestic market, and  $PQ_i$  stands for the price of domestic products.

*Income and Expenditure Block*

The behavior agents of the CGE model are made up of Chinese government, household, enterprises, and the rest of the world. The income of the Chinese government, however, is comprised of inhabitant income tax, corporate income tax, and transfer payments from the rest of the world. While the expenditure of the Chinese government is composed of four parts: government consumption, household transfer payments, enterprise transfer payment, and transfer payments for the rest of the world. Moreover, transfer payments from the government and the factor profit such as the capital factor earning or the labor remuneration constitute household income. Besides, the household expenditures obtained household consumption and their income tax. Another important agent is enterprise apart from the government and household. Its income, including capital revenue and energy factor, is profit. In contrast, the expenditure of the enterprise is divided into two parts: income tax for government and wages for workers. The relationship between each agent in this income and expenditure block could be described as in Fig. 2.

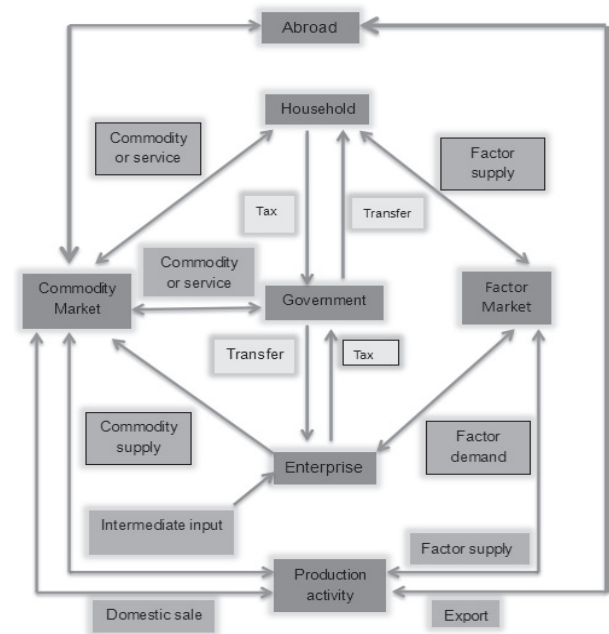


Fig. 2. Activity and behavior of each agent. Notes: the double-headed arrows mean that there are both commodities or factors and money or values to flow between the agents or markets. For example, the commodity market provide commodities or services to a household, while the household must pay for its consumption. This flow is bidirectional. In contrast, the single-direction arrows represent that there are only money or value to flow across the agents or markets. For example, households pay taxes for the government.

*Investment and Saving Block*

The total investment of our national economy is constituted by each sector's investment. With respect to each sector's investment, however, it is supposed to be exogenous. Gross saving is composed of household saving, enterprise saving, and government saving. Particularly, the government income minus the government expenditure equals government saving, while a unique saving system called net saving abroad is constituted by the difference of the quantity of import and the quantity of export.

*Pollution Abatement Block*

This block is formed by three sections and consists of four descriptive equations. The first part is about the carbon emissions of each production sector; the carbon emissions equal the total demand of each sectors' polluted energy multiplying carbon emission coefficients. Analogously, the quantitative relationship between SO<sub>2</sub> and NO<sub>x</sub> emissions is manifested in the second part, where QSD<sub>i</sub> represents the SO<sub>2</sub> emission of sector i (with a parallel meaning), QOD<sub>i</sub> stands for the NO<sub>x</sub> emission of sector i, and QH<sub>i</sub> means the residents consumption demand for the production of sector i. We put the concentration of PM<sub>2.5</sub> into the third part, where there exists a nonlinear function relation among these three variables, which include PM<sub>2.5</sub> concentration and SO<sub>2</sub> and NO<sub>x</sub> emissions. Where TOT<sub>pm2.5</sub> represents the concentration of PM<sub>2.5</sub>, coef<sub>i</sub>, g<sub>i</sub>, and k<sub>i</sub> are the coefficients of carbon, SO<sub>2</sub>, and NO<sub>x</sub> emissions. The concrete quantitative relationship is shown as equations (10) to (13).

$$CO_{2i} = coef_i * QRD_i \tag{10}$$

$$QSD_i = g_i * QH_i \tag{11}$$

$$QOD_i = k_i * QH_i \tag{12}$$

$$TOT_{pm2.5} = f(QSD_i + QOD_i) \tag{13}$$

*Household Welfare Block*

Household welfare is also called household utility because of the use of the equivalent variation as the standard to measure the variation trend of the household welfare. The index is shown in equation (14).

$$EV = e(p_0, u(QH_1)) - e(p_0, u(QH_0)) \tag{14}$$

...where P<sub>0</sub> expresses the household consumption goods' initial price, u(QH<sub>0</sub>) indicates the initial household consumption utility function, and u(QH<sub>1</sub>) represents the new household consumption utility function under policy shocking.

*Equilibrium and Macroeconomic Closures*

The equilibrium block consists of the equilibrium of the commodity market, the factor market, the trade market, investment, and savings. It is called neoclassicism macroeconomic closure, which we select as the macroeconomic closures in this CGE model. All

Table 1. Social accounting matrix in 2007 (billions of yuan).

		FA												
		A	C	L	EN	CA	H	E	G	T	Inv&Sav	F	SUM	
	A		242877									20403	263281	
	C	136974					47029		34350		44574		262927	
FA	L	68626											68626	
	EN	139											139	
	CA	57541											57541	
	H			68626		45541			-23952				90214	
	E				139	12000							12139	
	G						3186	8779		1433			13398	
	T		1433										1433	
	Inv&Sav						40000	3360	3000			-1787	44574	
	F		18616										18616	
	SUM	263281	262927	68626	139	57541	90214	12139	13398	1433	44574	18616	832888	

Notes: FA is factor, A is activity, C is commodity, L is labor, EN is energy, CA is capital, H is household, E is enterprise, G is government, T is tariff, Inv&Sav is investment and saving, F is foreign, SUM is the summary.

Table 2. Monthly average concentrations of PM<sub>2.5</sub> (ug/m<sup>3</sup>).

Date	Specific areas					average
	Nanjing	Guangzhou	Shanghai	Beijing	Ningbo	
2012-10	89.00	84.00	118.00	43.00	48.00	76.40
2012-11	194.00	49.00	50.00	72.00	56.00	84.20
2012-12	75.00	60.00	28.00	18.00	51.00	46.40
2013-01	205.00	74.00	26.00	69.00	50.00	84.80
2013-02	174.00	42.00	103.00	154.00	57.00	106.00
2013-03	48.00	35.00	57.00	226.00	57.00	84.60
2013-04	58.00	35.00	42.00	258.00	66.00	91.80
2013-05	164.00	10.00	18.00	20.00	48.00	52.00
2013-06	65.00	21.00	18.00	20.00	39.00	32.60
2013-07	23.00	33.00	88.00	11.00	39.00	38.80
2013-08	27.00	45.00	152.00	62.00	25.00	62.20
2013-09	59.00	53.00	150.00	90.00	28.00	76.00
2013-10	100.00	42.00	139.00	76.00	65.00	84.40
2013-11	136.00	50.00	203.00	31.00	39.00	91.80
2013-12	208.00	42.00	174.00	106.00	70.00	120.00
2014-01	30.00	54.00	41.00	14.00	53.00	38.40
2014-02	22.00	48.00	28.00	107.20	27.00	46.44
2014-03	26.00	56.00	17.00	44.70	59.00	40.54
2014-04	46.00	39.00	63.00	81.10	64.00	58.62
2014-05	76.00	54.00	61.00	26.90	41.00	51.78
2014-06	79.00	57.00	16.00	27.00	43.00	44.40
2014-07	72.00	74.00	136.00	133.10	43.00	91.62
2014-08	118.00	52.00	77.00	60.50	28.00	67.10
2014-09	226.00	12.00	88.00	53.30	41.00	84.06
2014-10	40.00	14.00	54.00	115.20	47.00	54.04
2014-11	36.00	23.00	18.00	52.90	46.00	35.18
2014-12	77.00	52.00	46.00	64.40	32.00	54.28
average	91.59	44.81	74.48	75.42	46.74	66.61

the prices (including factor price and commodity price) belong to the endogenous variables, although they are completely elastic. Furthermore, factor supplies such as labor and capital always equal the factor endowment, which represents full employment. In addition, we choose the labor price as the price benchmark, and make it 1.

#### The Recursive Dynamic Scheme

The recursive dynamic scheme of the CGE model employed in this paper is mainly through describing the changes of the labor growth and capital accumulation

during the dynamic period. It is shown as the following equations (15) and (16):

$$QLS_{t+1} = (1 + popg_t)QLS_t \quad (15)$$

$$QKS_{t+1} = (1 - deprete_t)QKS_t + QINV_t \quad (16)$$

...where  $popg_t$  is the growth rate of labor at time  $t$ ,  $deprete_t$  denotes the rate of depreciation at time  $t$ , and  $QINV_t$  represents the investment during the future period. Besides, the full time modeling frame is chosen to be 2016 to 2030.

Table 3. Scenario implementation plans.

Scenarios	Implementation		
	2016-20	2021-25	2025-26
Scenario 1	3.07% decline each year	3.07% decline each year	3.07% decline each year
Scenario 2	4.61% decline each year	1.53% decline each year	3.07% decline each year
Scenario 3	1.53% decline each year	4.61% decline each year	3.07% decline each year
Scenario 4	3.07% decline each year	4.61% decline each year	1.53% decline each year

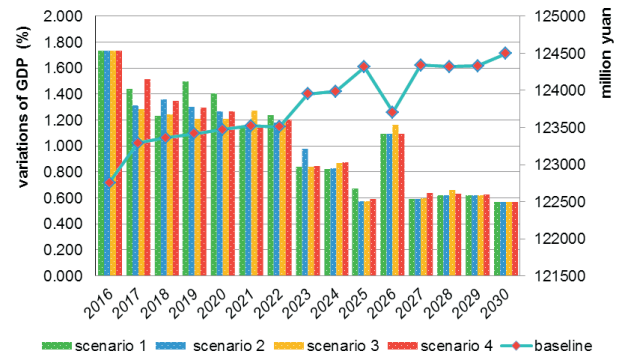


Fig. 3. Variation rate of GDP.

The Database

The database of this recursive dynamic CGE model is the Chinese 10 sectors macro society accounting matrix of 2007. The macro society accounting matrix is compiled based on the input-output table and the flow of fund statement.

Scenario Analysis

PM<sub>2.5</sub> concentration has been taken as an air pollution evaluating indicator into an environmental quality monitoring system by an increasing multitude of provinces and cities since 2012. In order to design the feasible scientific scenarios, we selected five regions' PM<sub>2.5</sub> concentrations as scenarios constituting the basis owing to their large capacity of data quantity: Nanjing,

Guangzhou, Shanghai, Beijing, and Ningbo. The average monthly PM<sub>2.5</sub> concentration, however, is shown in Table 2, as is the cities' daily average PM<sub>2.5</sub> concentration located at about 66.61 ug/m<sup>3</sup> since 2012 to 2014. Hence, the four scenarios are designed as shown in Table 3.

The Impacts on Macroeconomics

Gross domestic product (GDP), export, import, and household welfare are presented as macroeconomic criteria in this paper.

The influence on GDP under all of four scenarios demonstrates a consistent trend, which we can conclude from Fig. 3 and Table 4. Another coincident character by all the scenarios is that although the growth rate of the GDP decreases with each passing year, they still maintain a positive growth trend. An overall change trend of GDP

Table 4. Variation rates of GDP.

Year	Baseline (Millions of yuan)	Compared to baseline%			
		Scenario 1	Scenario 2	Scenario 3	Scenario 4
2016	122,756.7929	1.737	1.737	1.737	1.737
2017	123,289.8946	1.440	1.314	1.284	1.518
2018	123,359.7694	1.234	1.361	1.242	1.346
2019	123,418.8899	1.496	1.300	1.207	1.296
2020	123,471.9352	1.405	1.264	1.207	1.265
2021	123,522.7451	1.156	1.153	1.275	1.156
2022	123,506.0982	1.241	1.183	1.187	1.204
2023	123,949.956	0.840	0.978	0.842	0.846
2024	123,987.9972	0.823	0.828	0.871	0.877
2025	124,315.9849	0.670	0.577	0.577	0.591
2026	123,702.4573	1.094	1.095	1.165	1.096
2027	124,340.3377	0.591	0.591	0.599	0.641
2028	124,319.647	0.620	0.622	0.660	0.635
2029	124,332.3265	0.623	0.623	0.624	0.629
2030	124,494.6741	0.571	0.571	0.571	0.571

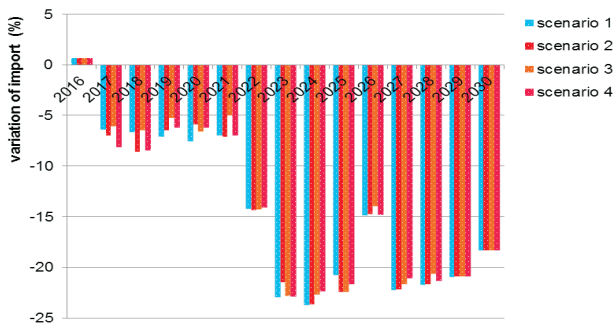


Fig. 4. Variation of imports.

under the influence of the four scenarios could be separated into three phases that involve a sharp drop, a sudden rise, and a slight decline, successively. A sharp drop means that all of the scenarios lead the growth rate of GDP to reduce progressively year by year before 2026. Scenario 1, however, manifests the least decrease with 0.67%, and the other three scenarios show almost the same percentage at about 0.58%. Afterward, a sudden rise emerges adjacent to the sharp drop. The growth rate of GDP increases abruptly in the year 2027 under the influence of all four scenarios, with scenario 3 rising the most quickly among all the scenarios as 1.165%; others show a similar rise with an average rate of 1.095%. In succession, the third variation trend assumes a slight decline, the difference between the sharp drop and slight decline is that the range of the slight decline after 2027 varies obviously lower than the sharp drop before 2026. Consequently, all four scenarios turn out to be the same condition with a percentage of 0.571% in 2030.

The variation trend of import presents a monotonous decline during the dynamic period. As a matter of fact, the import decline of 20.96% under scenario 1 becomes a mostly decreased scenario. In contrast, scenario 3 expresses the lowest decline with 20.88%, and the other two manifest a consistent tendency as an average percent of 20.91%. The variation trend is shown in Fig. 4.

The total change tendency of export under the influence of the four scenarios can be divided into two parts: a persistent decrease and a distinct recovery. The growth rate of export abated year after year from 2016 to 2025. The decline of export, as the variation trend shows,

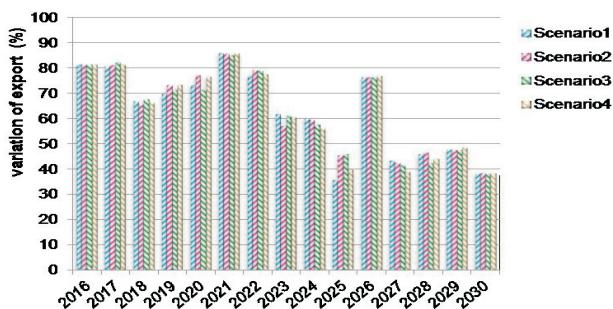


Fig. 5. Variation rate of exports.

appears the largest extent in 2025 under the influence of scenario 3, with a change percent of 46.27%; in contrast, the tiniest level of the decline in 2025 is caused by scenario 1, as 35.82%. In the next place, a distinct recovery arises from 2026. The mostly increasing variation of the export is under the effect of scenario 1 at 47.90%; in contrast, the lowest increase exists in scenario 3, at 47.66%. The concrete change data is shown in Fig. 5.

In principle, the tendency in Fig. 8 and Table 5 could be divided into two main types: positive and negative change. The positive variation periods transform from 2018 to 2020, 2025 to 2026, and 2029 to 2030. The household welfare obtains the greatest degree of improvement during 2018 to 2020, and scenario 1 contributes the greatest improvement to household welfare with a growth rate of 2.85%. In contrast, the negative variation period turns in the other years. The household welfare gets down to the maximum extent in 2026 to 2027, scenario 1, once again, retains the maximum extent of lessen with a decrease rate of 0.9384%.

### Impacts on Energy and the Environment

Carbon emission intensity and energy intensity are discussed as the evaluation indicators of energy and the environment.

The variation tendency of the carbon emission intensity is extremely unstable during the dynamic period that we can observe in Fig. 6. And it could be split into four stages. The first period varies from 2016 to 2019, and the carbon emission intensity holds a steady and slowly increasing character under the influence of all four scenarios during this time. Scenario 1 manifests the highest growth rate of 9.7% among all the other scenarios. Rapid growth appears in 2020 to 2022, meaning that each of the scenarios speeds up its growth rate and makes the carbon emission intensity increase significantly more quickly than before. Moreover, scenario 1 contributes the most increase to carbon emission intensity and possess a growth rate of 16.27%. Amazingly, each of the scenarios plummets during 2022 to 2024. Then a steady decrease dominates the variation trend after 2024, and it keeps this stable trend until 2030. It is worth mentioning that scenario 1, compared with the other three scenarios, suffered the most sensitive and prominent influence to the carbon emission intensity.

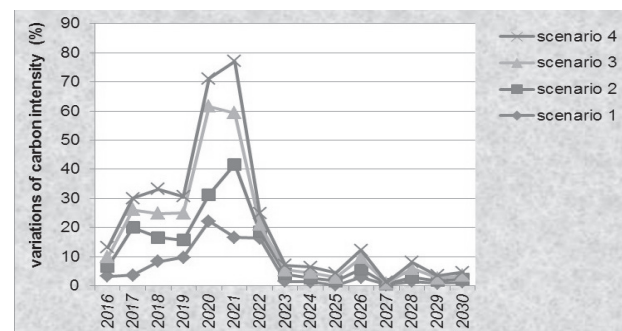


Fig. 6. Variation rate of carbon emission intensity.

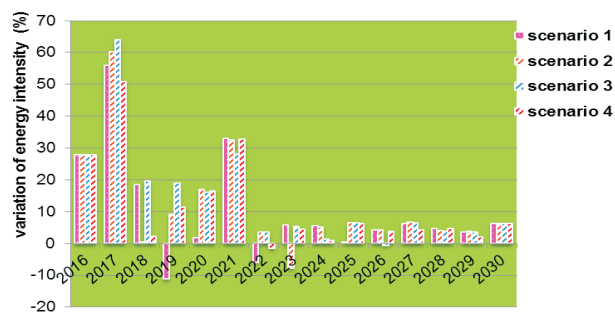


Fig. 7. Variation rate of energy intensity.

Generally speaking, energy intensity presents a periodic change tendency with its amplitude decreasing gradually during the dynamic variation years from Fig. 7. The maximum amplitude cycle appears in 2016 to 2019, and the peak value figures in 2017. Scenario 4 takes the highest peak value with a growth rate of 50.76%. Following the first cycle, the second cycle turns in 2020 and follows this circular development, the variation trend of the energy intensity holds this periodic change until 2030, yet the lowest valley value of all the scenarios occurs in 2030. Scenario 4, however, maintains the lowest valley value with a growth rate of 2.11%.

### The System Dynamics Model

#### The PM<sub>2.5</sub> Causality Diagram

The factors of which result in the formation of PM<sub>2.5</sub> originate broadly from different sources. Several factors

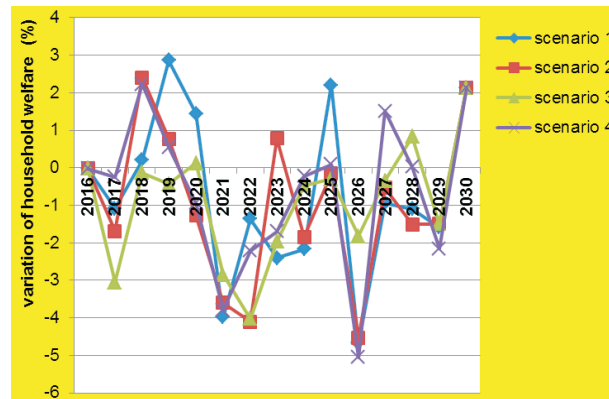


Fig. 8. Variation rate of household welfare.

have been corroborated according to scientific methods, for instance, fossil fuel burning in the manufacturing industries and power plants, fossil and biomass fuel burning for cooking and heating in the residential sector, garbage burning, and fugitive dust from road and domestic construction activities have been proven to be sources that can cause high PM<sub>2.5</sub> concentrations [37-39].

In view of the availability of data, we attribute these different formation causes into two major categories: primary emissions of fine particles and secondary emissions of fine particles. Primary emissions are issued from energy consumption – especially the fly ash of fuel and coal, oil fumes from the catering industry, and biomass combustion. Secondary emissions of fine particles are experienced from complicated chemical reactions such as SO<sub>2</sub> emissions, NO<sub>x</sub> emissions, smoke and dust emissions

Table 5. Variation rates of household welfare.

Year	Baseline (Millions of yuan)	Compared to baseline%			
		Scenario 1	Scenario 2	Scenario 3	Scenario 4
2016	55,562.22	-0.01757	-0.01757	-0.01757	-0.01757
2017	57,565.59	-1.08784	-1.6913	-3.05651	-0.24808
2018	55,552.92	0.197175	2.409269	-0.13495	2.220488
2019	56,067.81	2.858134	0.777533	-0.43561	0.552921
2020	56,603.48	1.443531	-1.27973	0.128357	-0.93933
2021	57,973.27	-3.97817	-3.59751	-2.85283	-3.78777
2022	57,799.4	-1.36297	-4.1076	-4.02432	-2.2173
2023	57,158.21	-2.40429	0.783336	-1.96687	-1.69492
2024	57,159.12	-2.16954	-1.84331	-0.46993	-0.22558
2025	56,180.38	2.206598	-0.1524	-0.29656	0.086697
2026	58,454.74	-4.6779	-4.524	-1.81899	-5.05597
2027	56,304.07	-0.9387	-0.53316	-0.35007	1.515548
2028	56,523.55	-1.09695	-1.51254	0.832965	0.025937
2029	56,629.79	-1.58414	-1.49307	-1.4953	-2.15828
2030	56,219.69	2.132108	2.132108	2.132108	2.132108

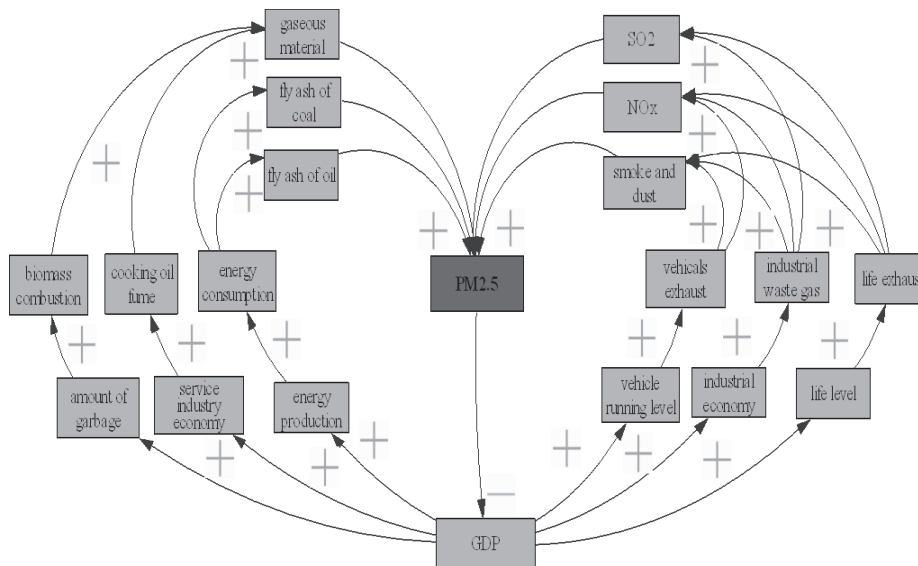


Fig. 9. Causality diagram of PM<sub>2.5</sub>.

from industrial waste gas emissions, exhausted emissions in life, and vehicle exhaust. In light of system dynamics theory, and according to these influenced factors, we establish the PM<sub>2.5</sub> causality diagram as Fig. 9 shows.

*The PM<sub>2.5</sub> System Flow Diagram*

A PM<sub>2.5</sub> system flow diagram that could manifested the quantitative relationship among flow variables, stock variables, auxiliary variables, and constant in accordance with the theory of difference equations and the principle of designing a flow diagram is shown in Fig. 10. Three stock variables, the amount of energy, PM<sub>2.5</sub> concentration, and industrial waste gas emissions are deployed. Energy production rate, energy consumption rate, the variation rate of PM<sub>2.5</sub> concentration, the industrial waste gas exhausted emissions, and the governing emissions of industrial waste gas also are denoted flow variables. Auxiliary variables and constant are also interpreted respectively. Correspondingly, the relationship among the main variables is demonstrated in the following equations (17) to (24).

$$CON_{pm2.5k} = CON_{pm2.5j} + RCON_{pm2.5} \times DT \tag{17}$$

$$RCON_{pm2.5} = \omega_1 \varphi_1 (ECR) + \omega_2 \varphi_2 (BCR) + \omega_3 \varphi_3 (COR) + \omega_4 \varphi_4 (IWGR) + \omega_5 \varphi_5 (MVER) + \omega_6 \varphi_6 (LWGR) \tag{18}$$

$$EA_k = EA_j + (EC - EP) \times DT \tag{19}$$

$$EC = coep \times FEP \times (OPA + CPA + NPA + EPA) \tag{20}$$

$$EP = coec \times FEC \times (OCA + CCA + NCA + ECA) \tag{21}$$

$$IWG_k = IWG_j + (IWGG - IWGP) \times DT \tag{22}$$

$$IWGP = EG_{so2} \times SR_{so2} + EG_{NOX} \times SR_{NOX} + SG \times SR_{SG} + DG \times SR_{DG} \tag{23}$$

$$IWGG = EXP(NPWG) + IOGG/UCGG \tag{24}$$

...where  $CON_{pm2.5k}$  represents the annual average concentration of PM<sub>2.5</sub> in year k,  $CON_{pm2.5j}$  represents the annual average concentration of PM<sub>2.5</sub> in year j,  $RCON_{pm2.5}$  is the variation change rate of PM<sub>2.5</sub> concentration, and  $DT$  stands for the difference step. Where  $ECR$  means the relationship between energy consumption and PM<sub>2.5</sub> concentration,  $BCR$  shows the relationship between biomass combustion and PM<sub>2.5</sub> concentration,  $COR$  is called the relationship between cooking oil fumes and PM<sub>2.5</sub> concentration,  $IWGR$  indicates the relationship between industrial waste gas emissions with PM<sub>2.5</sub> concentration,  $MVER$  means the relationship between monitoring vehicle exhaust and the PM<sub>2.5</sub> concentration, and  $LWGR$  is the exhausted emissions in life,  $\omega_i$ ; however, this all manifests the six influence factors' weight coefficient.

Where  $EA_k$  is short for the total amount of energy in year k,  $EA_j$  is the total amount of energy which represents the previous year k,  $EC$  means the energy consumption rate, and  $EP$  represents the energy production rate. Where  $FEP$  is called the influence factor of GDP per capita to energy production,  $OPA$  is known as the quantity of energy production in crude oil and  $CPA$  means the amount of energy production in raw coal; similarly,  $NPA$  and  $EPA$  show the total quantity of energy production in

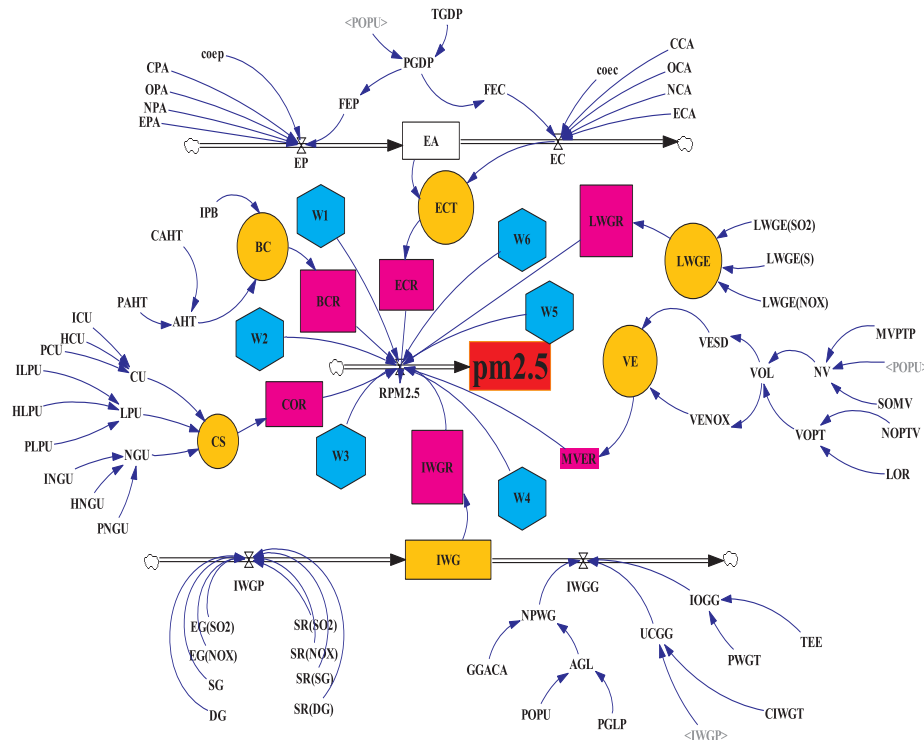


Fig. 10. System flow diagram.

natural gas and electric power separately, another constant *coep* conveys the production elasticity coefficient. And *FEC* delegates the relationship between GDP per capita and energy consumption during the process of energy consumption, *OCA* stands for the overall amount of energy consumption in crude oil, *CCA* represents the quantity of energy consumption in raw coal which has a parallel meaning as *NCA* and *ECA*, which demonstrates the total amount of energy consumption in natural gas and electric power respectively. And yet the constant *coec* manifests consumption elasticity coefficient.

Where  $IWG_k$  holds the meaning of industrial waste gas emissions in year *k*,  $IWG_j$  shows the industrial waste gas emissions in year *j* and which is the previous year *k*,  $IWGG$  represents the amount of the governing industrial waste gas emissions among the whole industrial waste gas exhausted emissions, and  $IWGP$  means the total industrial waste gas exhausted emissions. Where  $EG_{SO_2}$  shows the  $SO_2$  emissions during the industrial production progress,  $SR_{SO_2}$  is the standard rate of  $SO_2$  emissions during the industrial production progress,  $EG_{NO_x}$  is the  $NO_x$  emissions in the industrial producing process, and  $SR_{NO_x}$  manifests the standard rate of  $NO_x$  emissions, *SG* and *DG* represent the smoke emissions and dust emissions that the industry produces across their production process respectively.  $SR_{SG}$  and  $SR_{DG}$  however, demonstrate the standard rate of smoke and dust emissions during the industrial process. Where *NPWG* indicates the natural purification of the waste gas which originated from industrial emissions, *IOGG* means the investment on governing the industrial waste gas emissions, and *UCGG* represents the unit cost on industrial waste gas governing.

### System Simulation

The simulation interval is set from 2001 to 2030 and the simulation period is 30 years. Afterward, the difference step is one year. Consequently, this simulation is performed via Vensim software. Some main needed data is shown in Table 6.

We propose six countermeasures according to the six chief influence factors:

- 1) Increase the population that uses natural gas and liquefied petroleum gas; at the same time, decrease coal gas consumption; improve the natural gas consumption population from 21,207 million people to 25,000 million people, increase liquefied petroleum gas consumption from 15,682 million people to 20,000 million people, and decrease the coal gas consumption population from 2,442 million people to 2,000 million people.
- 2) Reduce industrial waste gas emissions; cut down the volume of industrial  $SO_2$  emissions from 1,775.82 million tons to 1,500 million tons, decrease the volume of industrial  $NO_x$  emissions from 1,580.81 million tons to 1,300 million ton,, reduce the industrial smoke emissions from 603.2 million tons to 500 million tons, and reduce industrial dust emissions from 448.7 million tons to 300 million tons.
- 3) Abate exhausted emissions in life; decrease life exhausted  $SO_2$  emissions from 205.665 million tons to 150 million tons, and  $NO_x$  emissions from 39.3123 million tons to 20 million tons, and smoke emissions from 142.673 million tons to 100 million tons.

Table 6. System dynamics simulation data.

Indicators	Pollutions (millions of tons)			Energy (millions of tons)	
	SO <sub>2</sub>	NO <sub>x</sub>	Smoke&Dust	Production	Consumption
Industry	1,911.7055	1,658.0515	1,029.3082	-	-
Life	205.6646	39.3123	142.6734	-	-
Vehicle	-	640.0293	63.6041	-	-
Crude oil	-	-	-	2.9534	6.8005
Raw coal	-	-	-	25.3863	24.0913
Natural gas	-	-	-	1.4269	1.881
Electric power	-	-	-	3.418	3.4002

- 4) Adjust the energy production and energy consumption structure, lower the amount of crude oil production and consumption as well as the quantity of raw coal production and consumption; decrease crude oil production from 2.9534 billion tons of standard coal to 2.5 billion tons of standard coal, as well as its consumption from 6.8005 billion tons of standard coal to 5 billion tons of standard coal, reduce the raw coal production from 25.3863 billion tons of standard coal to 20 billion tons of standard coal, as well as its consumption from 24.0913 billion tons of standard coal to 20 billion tons of standard coal.
- 5) Improve the proportion of harmless treatment garbage from 84.8% to 90%.
- 6) Decrease the emissions of vehicles exhaust; decrease the standard operating motor vehicles from 512,951 to 500,000 units.

In summary, six countermeasures can all lead to an adverse impact on PM<sub>2.5</sub> concentrations observed from Fig. 11 and Table 7. Consequently, countermeasures 2,

4, and 6 can approximately reach the target concentration of 35 ug/m<sup>3</sup> in 2030 with an average concentration of 33.85 ug/m<sup>3</sup>, 36.41 ug/m<sup>3</sup>, and 39.19 ug/m<sup>3</sup> respectively. Countermeasure 5, however, shows the weakest influence degree with an average level of 54.55ug/m<sup>3</sup>. Although countermeasures 1 and 3 manifest a higher influence degree than countermeasure 5, you could not yet reach the target.

### Results and Discussion

Scenario analysis in the CGE model demonstrated not only positive effects on the economy and welfare, but also negative effects on the environment and energy under the four PM<sub>2.5</sub> target plans. GDP, export, energy intensity, carbon emission intensity, and social welfare all appeared as unsteady and periodic variation trends that focused on 2020, 2025, 2026, and 2029. From the economic aspect, scenario 1 manifests the least decrease with 0.67% in GDP variation, declines the least 20.96% in import variation, and reaches the mostly increasing variation of exports with 47.90%. From the energy and environmental sphere, however, scenario 4 maintains the lowest valley value with a growth rate of 2.11%, and scenario 1 contributes the most increase in carbon emission intensity and possesses a growth rate of 16.27%. As the results show, setting up the implementation plan of PM<sub>2.5</sub> target as declining the PM<sub>2.5</sub> concentration at an annual average rate of 3.07% from 2016 to 2020, 4.61% from 2021 to 2025, and 1.53% from 2026 to 2030 may contribute to a more scientific and reasonable development in China. The system dynamic simulation results imply three effective countermeasures of realizing PM<sub>2.5</sub> targets. Reducing the industrial waste gas emissions, adjusting the energy production and energy consumption structures, and decreasing the emissions of vehicle exhaust could almost reach the PM<sub>2.5</sub> concentration target in 2030 with an average concentration of 33.85ug/m<sup>3</sup>, 36.41ug/m<sup>3</sup>, and 39.19ug/m<sup>3</sup>, which separately should attribute to the formation causes of PM<sub>2.5</sub>.

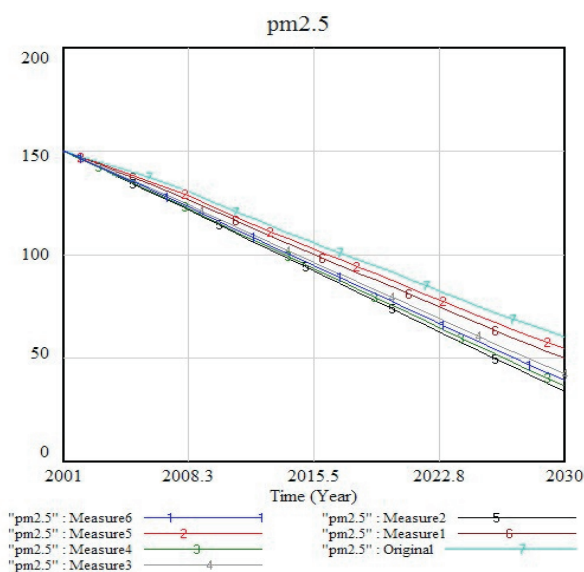


Fig. 11. Simulation results under different measurements.

Table 7. System dynamics simulation results (ug/m<sup>3</sup>).

Year	Original	Countermeasures					
		Measure1	Measure2	Measure3	Measure4	Measure5	Measure6
2016	104.027	98.2978	89.9265	94.3284	91.2477	100.838	92.7039
2017	100.865	94.8125	85.9162	90.5992	87.3225	97.5017	88.872
2018	97.7329	91.3454	81.9112	86.8814	83.4044	94.1883	85.049
2019	94.614	87.8859	77.9084	83.1683	79.4892	90.8847	81.2297
2020	91.447	84.3976	73.8972	79.4372	75.5629	87.5442	77.3963
2021	88.1941	80.8565	69.87	75.6727	71.6158	84.1368	73.5363
2022	84.8622	77.2653	65.8271	71.8758	67.6484	80.6669	69.6506
2023	81.4864	73.6458	61.7752	68.0604	63.6693	77.1618	65.7499
2024	78.1927	70.079	57.74	64.2793	59.7119	73.7223	61.8768
2025	74.9883	66.568	53.722	60.5339	55.7767	70.3529	58.032
2026	71.8821	63.1159	49.7214	56.8254	51.8643	67.0589	54.2164
2027	68.8847	59.7267	45.7385	53.1553	47.9752	63.8465	50.4308
2028	66.0094	56.4043	41.7736	49.5251	44.11	60.7229	46.6762
2029	63.1996	53.1163	37.8177	45.915	40.2566	57.6456	42.9371
2030	60.3759	49.8211	33.8599	42.3007	36.4007	54.5587	39.1947

### Conclusions

A multiple sector dynamic CGE model was constructed firstly in this study, and then four PM<sub>2.5</sub> implementation scenarios were designed for analyzing the impacts on China's macroeconomics, environment, and energy. Moreover, a PM<sub>2.5</sub> system dynamics model was established to reveal the influence factors and propose countermeasures to provide concrete suggestions for realizing the PM<sub>2.5</sub> target in 2030. With the results and discussions, some main findings are listed as follows:

1) To realize the PM<sub>2.5</sub> target in 2030, a decline in PM<sub>2.5</sub> concentrations at an annual average rate of 3.07% from 2016 to 2020, reduce PM<sub>2.5</sub> concentrations at an annual average rate of 4.61% from 2021 to 2025, and cut

down PM<sub>2.5</sub> concentrations at an annual average rate of 1.53% from 2026 to 2030 can therefore generally be a priority.

2) To reach the target more efficiently, decrease the total industrial waste gas emissions and reducing vehicle exhaust shall be considered. Cutting the volume of industrial SO<sub>2</sub> emissions to 1,500 million tons, decreasing the volume of industrial NO<sub>x</sub> emissions to 1,300 million tons, reducing industrial smoke to 500 million tons, abating industrial dust emissions to 300 million tons, and decreasing the standard operating motor vehicles to 50 million units from the current industrial and vehicle waste gas emission status might be the most efficiency strategy.

**Appendix:** Complete list of variables in casual loop diagrams.

Variable type	Variable	Description	Unit
Stock	PM <sub>2.5</sub>	The concentration of PM <sub>2.5</sub>	Ug/m <sup>3</sup>
	EA	The amount of energy	Million tce
	IWG	The industrial waste gas emissions	Million ton
Flow	RPM <sub>2.5</sub>	The variation rate of PM <sub>2.5</sub>	
	EP	Energy production rate	
	EC	Energy consumption rate	
	IWGG	The governing emissions of industrial	
	IWGP	The emissions from industry	

Auxiliary	ECT	Energy consumption	
	VE	Vehicles exhaust	
	BC	Biomass combustion	
	CS	Cooking smoke	
	LWGE	Waste gas from life	
	IWGR	The relationship between life waste gas and $PM_{2.5}$	
	COR	The relationship between cooking smoke and $PM_{2.5}$	
	MVER	The relationship between vehicles exhaust with $PM_{2.5}$	
	BCR	The relationship between biomass combustion with $PM_{2.5}$	
	ECR	The relationship between energy consumption with $PM_{2.5}$	
	LWGR	The relationship between life emissions of waste gas with $PM_{2.5}$	
	VESD	The emissions of smoke from vehicles exhaust	
	VENOX	The NOX emission from vehicles exhaust	
	VOL	The level of the vehicle operation	
	VOPT	The volume of passenger transport	10000 persontimes
	NV	Numbers of vehicles	Unit
	CU	The usage of coal	
	LPU	The usage of Liquefied petroleum gas	
	NGU	The usage of natural gas	
	AHT	Amount harmless treatment	
	NPWG	Natural purification of waste gas	
	AGL	Area of green land	
	UCGG	Unit cost of governing gas	
	IOGG	Investment on governing gas	
PGDP	GDP per capita		
CONSTANT	LWGE(SO2)	SO2 emissions from life	
	LWGE(NOX)	NOX emissions from life	
	LWGE(S)	Smoke emissions from life	
	MVPTP	Motor vehicles for public transport per 10000 population	Standard unit
	POPU	population	
	SOMV	Standard operating motor vehicles	Standard unit
	NOPTV	Number of public transport vehicles	unit
	LOR	Length of operating routes	km
	GGACA	Green covered area	%
	PGLP	Park green land per capita	Sq.m
	CIWGT	The cost of treat the industrial waste gas	
	PWGT	Proportion of the investment on governing the industrial gas	
	TEE	Total environment investment	
	IPB	Incineration proportion of garbage treatment	
	CAHT	The capacity of harmless treatment	
	PAHT	Proportion of harmless treatment	

CONSTANT	ICU	Industrial usage of coal	
	HCU	Household usage of coal	
	PCU	The usage population on coal	
	PNGU	The usage population on natural gas	
	INGU	Industrial natural gas usage	
	HNGU	Household usage of natural gas	
	PLPU	The usage population of Liquefied petroleum	
	HLPU	Household usage of Liquefied petroleum	
	ILPU	Industrial usage of Liquefied petroleum	

### Acknowledgements

This study is supported by the National Social Science Foundation of China (NSSFC) (grant No. 15BGL145), the National Natural Science Foundation of China (NSFC) (grant No. 71471061), the Fundamental Research Funds for the Central Universities (No. 2015ZD33), and the Center for Innovation Development and Energy Economics Research, North China Electric Power University.

### References

1. WANG K, WEI Y.M. China's regional industrial energy efficiency and carbon emission abatement costs. *Applied Energy* [J], **130**, 617, **2014**.
2. MICHEL D.E., HANNA F, NIKLAS H, ANNEMIEK A, NICKLAS F, ANDRIES F. H., JOS G.J., MARK R, HELEEN V.S. Greenhouse gas emissions from current and enhanced policies of China until 2030: Can emissions peak before 2030? *Energy Policy*[J], **89**, 224, **2016**.
3. MEHMET C. Determining the bioclimatic comfort in Kastamonu City. *Environmental Monitoring and Assessment*[J], **187**, 640, **2015**.
4. HAKAN S., MEHMET C., NUR B. Effects of Forests on Amounts of CO<sub>2</sub>:Case Study of Kastamonu and Ilgaz Mountain National Parks. *Polish Journal of Environmental Studies*[J], **24** (1), 253, **2015**.
5. MEHMET C., HAKAN S. Measuring the Impact of Selected Plants on Indoor CO<sub>2</sub> Concentrations. *Polish Journal of Environmental Studies*[J], **25** (3), 973, **2016**.
6. MEHMET C. A Change in the Amount of CO<sub>2</sub> at the Center of the Examination Halls: Case Study of Turkey. *Ethno Med*[J], **10** (2), 146, **2016**.
7. YASMANY M., PIERRE H., MATTHEW P.F., ALBERTO M. Secondary organic aerosol contributions to PM<sub>2.5</sub> in Monterrey, Mexico: Temporal and seasonal variation. *Atmospheric Research*[J], **153**, 348, **2015**.
8. BRADLEY B. Pedestrian exposure to near-roadway PM<sub>2.5</sub> in mixed-use urban corridors: A case study of Omaha, Nebraska. *Sustainable Cities and Society*[J], **15**, 64, **2015**.
9. AMOD K.P., MICHAEL N.B, JIWAN A, PALLE V, RAM K.C., PRAKASH S.S., ANIL K.R., KIRK R.S. PM<sub>2.5</sub> in household kitchens of Bhaktapur, Nepal, using four different cooking fuels. *Atmospheric Environment*[J], **113**, 159, **2015**.
10. WANG J., LI X., JIANG N., ZHANG W.K., ZHANG R.Q., TANG X.Y. Long term observations of PM<sub>2.5</sub>-associated PAHs: Comparisons between normal and episode days. *Atmospheric Environment*[J], **104**, 228, **2015**.
11. MAURO M., STEFANIA S., GIANCARLO R., BRUNO P. Source apportionment of PM<sub>2.5</sub> at multiple sites in Venice (Italy): Spatial variability and the role of weather. *Atmospheric Environment*[J], **98**, 78, **2014**.
12. WANG D.X., HU J.L., XU Y., LV D., XIE X.Y., MICHAEL K., XING J., ZHANG H.L., YING Q. Source contributions to primary and secondary inorganic particulate matter during a severe wintertime PM<sub>2.5</sub> pollution episode in Xi'an, China. *Atmospheric Environment*[J], **97**, 182, **2014**.
13. RAY M., KATE B., FRANCISCO P.S. Alignment of policies to maximize the climate benefits of diesel vehicles through control of particulate matter and black carbon emissions. *Energy Policy*[J], **54**, 54, **2013**.
14. YUE X., WU Y., HAO J.M., PANG Y., MA Y., LI Y., LI B.S., BAO X.F. Fuel quality management versus vehicle emission control in China, status quo and future perspectives. *Energy Policy*[J], **79**, 87, **2015**.
15. MIKUŠKA P., KRŮMAL K., VEČEŘA Z. Characterization of organic compounds in the PM<sub>2.5</sub> aerosols in winter in an industrial urban area. *Atmospheric Environment*[J], **105**, 97, **2015**.
16. WANG Y.G., YING Q., HU J.L., ZHANG H.L. Spatial and temporal variations of six criteria air pollutants in 31 provincial capital cities in China during 2013-2014. *Environment International* [J], **73**, 413, **2014**.
17. WU C.F., LIN H.I., HO C.C., YANG T.H., CHEN C.C., CHAN C.C. Modeling horizontal and vertical variation in intraurban exposure to PM<sub>2.5</sub> concentrations and compositions. *Environmental Research*[J], **133**, 96, **2014**.
18. CHENG Y., HE H.B., DU Z.Y., ZHENG M., DUAN F.K., MA Y.L. Humidity plays an important role in the PM<sub>2.5</sub> pollution in Beijing. *Environmental Pollution*[J], **197**, 68, **2015**.
19. NATHANIEL G., SUSAN E.P. Residential demand response reduces air pollutant emissions on peak electricity demand days in New York City. *Energy Policy*[J], **59**, 459, **2013**.
20. ZHAO Y.L., LIN Z.Q., JIA R.H., LI G.J., XI Z.G., WANG D.Y. Transgenerational effects of traffic-related fine particulate matter (PM<sub>2.5</sub>) on nematode *Caenorhabditis elegans*. *Journal of Hazardous Materials* [J], **274**, 106, **2014**.
21. MICHAL P.S, GABRIELA D.K., BARBARA K., MARIE F., STEFFEN L., LARS G. Evaluation of building characteristics in 27 dwellings in Denmark and the effect of using particle filtration units on PM<sub>2.5</sub> concentrations. *Building and Environment* [J], **73**, 55, **2014**.
22. LI J.H. The introduction of IO and CGE model. IO and CGE model applied to the study of macroeconomics [M].

- Shanghai University of Finance and Economics press, China, **1**, 2, **2013**.
23. VIRGINIE D., JEAN-MARC P., CRISTINA S. Biofuels, tax policies and oil prices in France: Insights from a dynamic CGE model. *Energy Policy [J]*, **66**, 603, **2014**.
  24. ASBJØRN A., BÅRD R., WEI T.Y., JÓN E.K., HELENE M., ULRIKE N., HAUKE S. An economic evaluation of solar radiation management. *Science of The Total Environment [J]*, **532**, 61, **2015**.
  25. ARSHAD M., CHARLES O.P.M. Carbon pricing and energy efficiency improvement – why to miss the interaction for developing economies? An illustrative CGE based application to the Pakistan case. *Energy Policy[J]*, **67**, 87, **2014**.
  26. CLAUDIA H., ANDREAS L., TIM M. A new robustness analysis for climate policy evaluations: A CGE application for the EU 2020 targets. *Energy Policy [J]*, **55**, 27, **2013**.
  27. SUTHIN W., JOHN A.A. Is there a role for biofuels in promoting energy self sufficiency and security? A CGE analysis of biofuel policy in Thailand. *Energy Policy[J]*, **55**, 543, **2013**.
  28. JOHANNES B. The value of air pollution co-benefits of climate policies: Analysis with a global sector-trade CGE model called WorldScan. *Technological Forecasting and Social Change[J]*, Part A, **90**, 178, 2015.
  29. TAO J., ZHANG L.M., ZHANG Z.S., HUANG R.J., WU Y.F., ZHANG R.J., CAO J.J., ZHANG Y.H. Control of PM<sub>2.5</sub> in Guangzhou during the 16<sup>th</sup> Asian Games period: Implication for hazy weather prevention. *Science of the Total Environment [J]*, **508**, 57, **2015**.
  30. ALEJANDRA S., ALEJANDRO D.G. Proposals to enhance thermal efficiency programs and air pollution control in south-central Chile. *Energy Policy [J]*, **79**, 48, **2015**.
  31. SUN J., JEREMY S., WANG J., JOSHUA S.F., WANG S.X. Cost estimate of multi-pollutant abatement from the power sector in the Yangtze River Delta region of China. *Energy Policy[J]*, **69**, 478, **2014**.
  32. SANTIAGO M., LUIS J.M., BLÁZQUEZ L.F. A system dynamics approach for the photovoltaic energy market in Spain. *Energy Policy [J]*, **60**, 142, **2013**.
  33. JUNESEUK S., SHIN W.S., LEE C.Y. An energy security management model using quality function deployment and system dynamics. *Energy Policy [J]*, **54**, 72, **2013**.
  34. ALI KEREM S., MUSTAFA H. Exploring the options for carbon dioxide mitigation in Turkish electric power industry: System dynamics approach. *Energy Policy [J]*, **60**, 675, **2013**.
  35. YU S.W., WEI Y.M. Prediction of China's coal production-environmental pollution based on a hybrid genetic algorithm-system dynamics model. *Energy Policy[J]*, **42**, 521, **2012**.
  36. HAMED V.A., SALMAN J., HOSSEIN D., JAFAR H., SAEED M. A system dynamics modeling for urban air pollution: A case study of Tehran, Iran. *Transportation Research Part D[J]*, **31**, 21, **2014**.
  37. SARATH K.G., DINESH M. Re-fueling road transport for better air quality in India. *Energy Policy[J]*, **68**, 556, **2014**.
  38. ALEXANDER G., CRISTIÁN M.M. Wind, coal, and the cost of environmental externalities. *Energy Policy[J]*, **62**, 1385, **2013**.
  39. TOMMI E., NIKO K., JARKKO T., LAURA S., KAARLE K., OLLI S., MIKKO S., JORMA J., ILKKA S. A multi-criteria analysis of climate, health and acidification impacts due to green house gases and air pollution – The case of household-level heating technologies. *Energy Policy [J]*, **74**, 499, **2014**.